Computer Simulation of Small Molecule Permeation across a Lipid Bilayer: Dependence on Bilayer Properties and Solute Volume, Size, and Cross-Sectional Area

D. Bemporad,* C. Luttmann,† and J. W. Essex*
*School of Chemistry, University of Southampton, Highfield, Southampton, United Kingdom; and †Aventis Pharma SA, Vitry sur Seine, France

ABSTRACT Cell membrane permeation is required for most drugs to reach their biological target, and understanding this process is therefore crucial for rational drug design. Recent molecular dynamics simulations have studied the permeation of eight small molecules through a phospholipid bilayer. Unlike experiments, atomistic simulations allow the direct calculation of diffusion and partition coefficients of solutes at different depths inside a lipid membrane. Further analyses of the simulations suggest that solute diffusion is less size-dependent and solute partitioning more size-dependent than was commonly thought.

INTRODUCTION

For most of the routes of administration, drugs have to cross cell membranes to reach the general circulation. Even after direct injection, or even if the drug can permeate via the paracellular route in the extracellular space, it soon encounters cell membranes to be crossed to reach its biological target inside the cell cytoplasm. Unless they are analogs of physiological substrates, drugs commonly cross cell membranes by passive permeation without the help of protein carriers. An understanding of solute partitioning into biological membranes is then crucial for subcellular pharmacokinetics and rational drug design (Balaz, 2000).

Functional cell membranes are fluid mosaics of proteins within a lipid bilayer matrix (Singer and Nicolson, 1972). Experimental and theoretical models for biological membranes, especially when studying solute permeation, are therefore phospholipid bilayers. Among them, extensive data have been collected for the dipalmitoylphosphatidylcholine (DPPC) bilayer.

For small organic molecules, experimental techniques have been developed to measure directly their permeability coefficient across planar phospholipid bilayers separating two chambers (Bean et al., 1968; Walter and Gutknecht, 1984, 1986; Wolosin and Ginsburg, 1975; Finkelstein, 1976; Orbach and Finkelstein, 1980; Brunner et al., 1980; Gutknecht and Walter, 1981) or across phospholipid bilayers forming large unilamellar vesicles (Brunner et al., 1980; Bar-On and Degani, 1985; Bochain et al., 1981; Lande et al., 1995; Xiang and Anderson, 1995, 1997, 1998b,c, 2000a,b; Bresseleers et al., 1984; Dix et al., 1978). Experimental data are interpreted with the so-called solubility-diffusion model of permeation (Cohen, 1975a,b; Wolosin and Ginsburg, 1975; Finkelstein, 1976; Diamond and Katz, 1974; Orbach and Finkelstein, 1980; Todd et al., 1989; Xiang and Anderson, 1997, 1998a,b, 2000a; Lande et al., 1995; Paula et al., 1996; Hill et al., 1999). The overall membrane resistance R to solute permeation, defined as the inverse of the permeability coefficient P, can be expressed as the integral over the local resistances across the membrane (Berendsen and Marrink, 1993; Xiang and Anderson, 1994, 1998a, 2000a):

$$R = \frac{1}{P} = \int_0^{\mathrm{d}} \frac{dz}{K(z)D(z)}. \tag{1}$$

Here $K(z)$ and $D(z)$ are the depth-dependent partition coefficient from water into the membrane and the diffusion coefficient in the membrane at depth z, respectively, and d is the membrane thickness. Assuming, however, that transport is governed primarily by a distinct and uniform barrier region within the membrane, the above equation simplifies to (Xiang and Anderson, 1994, 1998a, 2000a),

$$R = \frac{d_{\mathrm{barrier}}}{K_{\mathrm{barrier}}D_{\mathrm{barrier}}} = \frac{1}{P^{\mathrm{m}}}, \tag{2}$$

where K_{barrier} and D_{barrier} are the solute partition coefficient from water into, and the solute diffusion coefficient through, the barrier region of the membrane, and d_{barrier} is the thickness of the barrier domain.

The value of D_{barrier} is not accessible from experiments and is sometimes approximated to the diffusion coefficient of the solute under study in water or organic solvents (Xiang et al., 1992; Xiang and Anderson, 1998b; Finkelstein, 1976; Orbach and Finkelstein, 1980). Also the value of K_{barrier} cannot be obtained from experiments of water/membrane partitioning, since the zone of solute maximum partition accounts for only a small fraction of the resistance to permeation and that of minimum partition accounts disproportionately for the resistance, as a solute tends to partition

Submitted June 30, 2003, and accepted for publication February 4, 2004.

Address reprint requests to J. W. Essex, School of Chemistry, University of Southampton, Highfield, Southampton SO17 1BJ, UK. Tel.: 44 (0) 23-8059-2794; Fax: 44 (0) 23-8059-3781; E-mail: jwel@soton.ac.uk.

0006-3495/04/07/1/13 $2.00

doi: 10.1529/biophysj.103.030601

into that region with the lowest solvation energy rather than into the barrier domain. Fair correlations were obtained between the measured P^m and the solute partition coefficient in reference organic solvents, K_{org}, which are commonly chosen among 1-octanol or long-chain alkanes or alkenes because of the hydrocarbon nature of the lipid bilayer core. This was first observed with anesthetic compounds and lead Overton at the end of the 19th century to state an empirical rule according to which solute permeation through biological membrane is proportional to its partition in water/oil systems (Overton, 1895). Today, it is well known that biomembranes differing in lipid composition, temperature, and level of hydration require different reference organic solvents.

Molecular dynamics (MD) simulation is a powerful technique yielding atomic details which are not available in experiments.

The use of MD simulations to study aspects of solute diffusion through lipid bilayer membranes was applied first by Stouch and co-workers (Bassolino-Klimas et al., 1995, 1993; Stouch et al., 1995; Alper and Stouch, 1995). They calculated the diffusion coefficient D from the solute mean-squared displacement in different regions of the hydrocarbon core of the membrane. Results of simulations with benzene molecules in a DMPC bilayer showed that the diffusion is higher in the middle of the membrane than closer to the lipid headgroups and that this behavior paralleled the distribution of free volume and the lipid chain *trans*/*gauche* interconversion rates. The mechanism of diffusion was revealed: benzene molecules rattled around in a particular void for a relatively long period of time, and took infrequent jumps to another void. Simulations with a drug analog showed instead that the diffusion coefficient for larger molecules does not vary at different positions in the membrane and that hydrogen bonds played an important role in determining the solute orientation (Alper and Stouch, 1995). The mean-squared displacement was also calculated for benzyl-alcohol (Cascales et al., 1998) and halothane (Tu et al., 1998; Koubi et al., 2000) by other workers, but the main goal of those studies was to investigate the modifications induced by the anesthetic on the lipid bilayer structure. The relationship between solute polarizability and size on the one hand, and free energy of solute transfer from water into membrane models on the other, has been studied and reviewed extensively by Pohorille and co-workers (Pohorille and Wilson, 1996; Pohorille et al., 1999; Pratt and Pohorille, 2002). The free energy of solute transfer from the water phase into the membrane was calculated for various anesthetic compounds with the particle insertion method or Umbrella sampling. They found that the work to create a cavity able to locate a permeant solute is lower inside the membrane than in water, whereas the electrostatic contribution to the solute transfer increases monotonically going from water into the membrane interior. A balance between these two opposite effects causes dipolar compounds to accumulate at the water/membrane interface, whereas apolar compounds resided predominantly in the membrane core. This behavior was qualitatively related to the anesthetic power of these compounds, with the most polar that concentrate at the interface being the most powerful (Pratt and Pohorille, 2002).

The first complete study of the permeation process by MD simulations is by Marrink and Berendsen (1994, 1996). By simply constraining the solute molecules at given depths inside a lipid bilayer and calculating the force required to maintain the position constraint, both solute local diffusion coefficients at those depths and free energies of solute partitioning from water to those depths were calculated. Combining the two physical quantities, the overall permeation coefficient was obtained according to Eq. 1. This method was applied to water, ammonia, and oxygen molecules. The particle insertion method was also applied by Marrink and Berendsen (1996) to a series of Lennard-Jones particles of various sizes and shapes. In the membrane center (low lipid density) the difference in size did not affect significantly the solute partitioning behavior, whereas along the upper part of the lipid tails (high lipid density) a steep size-dependence was found. Regarding solute asphericity, elongated particles were somewhat stabilized along the upper part of the lipid tails, where pockets of free space have an elongated shape that parallel the lipid molecules.

Recently, several nanosecond-long all-atom MD simulations have been performed (Bemporad et al., 2004) investigating the permeation process of eight small organic compounds in a DPPC bilayer membrane. The eight solutes represent the most common chemical functional groups: acetamide, acetic acid, benzene, ethane, methanol, methylacetate, methylamine, and water. The same simulation method first introduced by Marrink and Berendsen (1994) was employed for these simulations. The solutes under study were constrained at different depths inside the lipid bilayer and this methodology allowed the calculation of the force acting on the center of mass of the solutes at different distances from the bilayer center along the bilayer normal. The free energy of solute partitioning was obtained by integrating the mean force along the bilayer normal (reaction coordinate), and the local diffusion coefficient was obtained from the time autocorrelation function of the fluctuations of the instantaneous force from its time average. Resistance and permeability coefficients were calculated from these data by applying Eq. 1 directly. Simulation results compared favorably with available experimental data and previous simulations.

Further analyses of these simulations are presented here. Whereas the previous article (Bemporad et al., 2004) focused on the calculation of the relevant physical properties, the aim of this article is to investigate the possible correlations between such properties and the molecular behavior of both lipids and solutes, and also possible similarities or dissimilarities between the bilayer membrane and bulk liquids.

SIMULATION PROTOCOL

The simulation box consisted of a 2×36 DPPC bilayer with 2094 water molecules (full hydration). An equilibrated starting structure of the lipid bilayer was kindly obtained from A. D. MacKerell and S. E. Feller. Lipids, water, and the eight organic solutes were modeled using the latest CHARMM force field for lipids and proteins. The simulation protocol was the same as that used in some of Feller's latest simulations (MacKerell and Feller, 2000; Feller et al., 1997). The Lennard-Jones (LJ) potential was switched smoothly to zero between 10 and 12 Å. Electrostatic interactions were calculated with the particle-mesh Ewald method with a κ-value of 0.23 and a fast-Fourier grid density of ~ 1 Å^{-1}. The real space part of the particle-mesh Ewald summation was truncated at 12 Å. All covalent bonds involving hydrogens were constrained using the SHAKE algorithm (Ryckaert et al., 1977). The equation of motion was solved employing the leap-frog algorithm (Hockney, 1970) with a 2-fs time step. A distance of 14 Å was used for the neighbor list, which was updated every 50 fs. Coordinates were saved every picosecond for subsequent analysis. Three-dimensional periodic boundary conditions were applied. Only the cell length normal to the membrane was allowed to vary during the simulation to maintain a constant normal pressure (P_N) of 1 atm. The cell dimensions defining the membrane plane were kept fixed to maintain a constant surface area per lipid (A) of 62.9 Å^2. The pressure was maintained by the Langevin piston algorithm (Feller et al., 1995) with a mass of 500 a.m.u. and a collision frequency of 5 ps^{-1}. The Hoover thermostat (Hoover, 1985) was used to maintain the temperature (T) at 50°C, well above the phase transition temperature of DPPC bilayers, with a value of 1000 kcal ps^2 for the thermostat (fictitious) mass. The ensemble was therefore NP_NAT. The eight solutes studied were free to move on the x,y plane, but constrained at chosen distances from the bilayer center using the so-called z-constraint algorithm (Marrink and Berendsen, 1994, 1996). In such an algorithm, a solute is placed at a chosen z-depth in the membrane The force acting on its center of mass at each time step, $\mathbf{F}(z, t)$, is obtained as the negative of the force required to maintain the z-coordinate of the center of mass constrained at that z-depth. Eventually, the free energy difference $\Delta G(z)$ between the water phase (outside the membrane) and depth z is accessible as the potential of the mean force:

$$\Delta G(z) = -\int_{\text{outside}}^{z} \langle \mathbf{F}(z') \rangle_t dz'. \quad (3)$$

In this equation, $\langle \ldots \rangle_t$ indicates average over the simulation time. The free energy difference is related to the solute partition coefficient $K(z)$ between water and depth z:

$$K(z) = \exp(-\Delta G(z)/RT). \quad (4)$$

The local diffusion coefficient of the solute at depth z is also obtained from $\mathbf{F}(z, t)$:

$$D(z) = \frac{RT}{\tilde{\xi}} = \frac{(RT)^2}{\int_0^\infty \langle \Delta\mathbf{F}(z,t) \cdot \Delta\mathbf{F}(z,0) \rangle dt}. \quad (5)$$

Finally, $\Delta G(z)$ and $D(z)$ allow for the calculation of the local resistances R(z), whose integration along the bilayer normal yields the overall resistance R to permeation, according to the solubility-diffusion model:

$$R = \int_{\text{outside}}^{z} R(z')dz' = \int_{\text{outside}}^{z} \frac{\exp(\Delta G(z')/RT)}{D(z')} dz'. \quad (6)$$

The permeability coefficient P of the solute is defined as the inverse of R (see Eq. 1).

The small organic molecules were manually inserted in the lipid bilayer at the desired z-depth and a crude short minimization was performed to eliminate bad contacts. The steepest descent algorithm was employed for the minimizations. For each of the eight molecules, 10 z-depths were sampled in the region 0–30.5 Å from the bilayer center. Then, each simulation was run for 2.1 ns, with the first 100 ps discarded as equilibration. Results from one leaflet of the lipid bilayer were considered valid for the other layer too, for reasons of symmetry. For each z-depth, five x,y positions on the bilayer plane were sampled. In each single simulation, five z-depths (out of 10) were studied at the same time, i.e., each simulation contained five solutes constrained at five different z-depths and x,y locations. This leads to a total of 10 simulations for each molecule. Starting positions for the solutes were chosen with care to avoid solute-solute interactions and clustering. Therefore, for each molecule, P was calculated from 20 ns of simulations and for the eight molecules a total of 160 ns of data collection was performed.

Although experiments clearly show that lipid bilayers are tension-free, supporting the use of an isotropic pressure ensemble in MD simulations, it has been argued that a nonzero surface tension (γ) is appropriate to correct for the finite size of the simulation system compared with macroscopic real membranes whose experimental properties are to be reproduced (Feller and Pastor, 1996). It has been shown that with the CHARMM force field a constant nonzero surface tension ensemble ($NP_N\gamma T$) or a constant surface area per lipid ensemble (NP_NAT) yield the best agreement with experiments (Feller et al., 1997; Feller and Pastor, 1999) and are equally reliable. For this reason a ''simpler'' NPT ensemble seemed inappropriate for these simulations. A fully flexible simulation cell in the $NP_N\gamma T$ ensemble could therefore be chosen for these permeation studies. Unfortunately, there is no guiding procedure for obtaining the appropriate value of γ for the size, the force field and, in this case, the presence of solutes in the lipid

bilayer under study. Previous work (Feller and Pastor, 1999) demonstrates that convergence and sufficient sampling of area fluctuations would require tens of nanoseconds for fairly precise determinations of the value for γ. Furthermore, the CHARMM authors prefer using a constant surface area rather than constant surface tension ensemble in their work on lipid bilayers. The final choice of ensemble for these simulations was therefore NP_NAT. When a small amount of a small solute enters the membrane, the overall lipid structure is not altered, as shown by these and previous simulations, so that the area per lipid should also arguably remain constant. Moreover, the same packing constraints existing in pure lipid membranes are expected to still act when solutes try to permeate: these studies were not intended to understand modifications to lipid structure by solutes, but rather the forces operating on solutes while permeating the membrane. However, we are aware that the bilayer surface area may increase slightly on penetration of the headgroup region by the solutes, and consequently care was taken to ensure that only one solute was present in the densest region of the bilayer for each leaflet at any one time.

All the simulations were run in parallel with four processors, using version 27 of the CHARMM software package (Brooks et al., 1983). A few simulations were run on a cluster of PCs with 750-Mhz AMD Athlon processors, but most were run on a cluster of PCs with 1000-Mhz Intel Pentium IIIs and 1500-Mhz Intel Pentium IVs.

FOUR-REGION MODEL

Since the membrane has a very inhomogeneous character when moving from one side to the other, each individual layer has been split into four regions as described in previous publications (Marrink and Berendsen, 1994, 1996):

Region 1: low headgroup density, 20 to 27 Å from the bilayer center.
Region 2: high headgroup density, 13 to 20 Å from the bilayer center.
Region 3: high tail density, 6 to 13 Å from the bilayer center.
Region 4: low tail density, 0 to 6 Å from the bilayer center.

The same distinction between membrane regions has been adopted here in the interpretation of the permeation results.

BILAYER/BULK SOLVENT COMPARISONS

As mentioned in the Introduction, in experiments the measured permeability coefficients are commonly related to the partition coefficients of the solutes under study in various reference organic solvents. This is because the solute partition coefficient from water into the membrane barrier domain cannot be obtained. From simulations, however, the solute partition coefficient at different depths inside the lipid bilayer can be obtained from the calculated free energies (see Eq. 4), allowing direct comparisons to be made.

Selectivity coefficients

The selectivity coefficient s between solute partition K into two different solvents X and Y is defined as (Katz et al., 1983; Xiang and Anderson, 1998a):

$$\log K(X) = s \log K(Y) + r. \tag{7}$$

When the two solvents yield $s = 1$, they show identical chemical selectivity toward the solutes under study. If $K(X)$ is taken to be the partition coefficient in the lipid bilayer, correlations between the latter and reference organic solvents Y can be studied. The solvent yielding s closest to 1 is considered to be the solvent that best mimics the barrier domain of the permeation process. The correlation between the experimental partition coefficients in water/hexadecane systems, $K(\text{water} \rightarrow \text{hexadecane})$, and the calculated partition coefficients at different depths in the lipid bilayer, $K(z)$, has been studied by plotting log $K(z)$ versus log $K(\text{water} \rightarrow \text{hexadecane})$ (graphs not shown). Since in drug design water/1-octanol partition coefficients are widely used to estimate drug ability to permeate cell membranes, log $K(z)$ versus log $K(\text{water} \rightarrow \text{octanol})$ plots have also been examined. This solvent is commonly considered a good model for the biomembrane chemical environment because of the presence of a polar head and a hydrocarbon chain. The gradients of such log-log plots correspond to the selectivity coefficients s between the reference organic solvents and the lipid bilayer. The relevant results are reported in Table 1.

Considering hexadecane, the best (highest correlation coefficient) and most linear (slope closest to unity) correlation is at $z = 3$ Å and the second most linear correlation is at $z = 0$ Å. This was expected, because hexadecane has a similar chemical nature to that of region 4 of the lipid bilayer. Considering 1-octanol, the most linear correlation is shifted toward the interface and is located at $z = 9.5$ Å; at this depth the correlation coefficient is also

TABLE 1 Correlation between calculated partition coefficients at different *z*-depths in the bilayer and experimental partition coefficients in water/hexadecane and water/octanol systems

		Water/hexadecane		Water/octanol	
Bilayer regions	z-depth/Å	Slope	Correlation coefficient	Slope	Correlation coefficient
2	16.5	0.11	0.64	0.21	0.64
2/3	13.0	0.32	0.88	0.61	0.88
3	9.5	0.54	0.93	1.01	0.92
3/4	6.0	0.71	0.95	1.31	0.93
4	3.0	0.77	0.95	1.41	0.92
4	0.0	0.76	0.93	1.38	0.90

Experimental partition coefficients are from Zhu et al. (1998) and Walter and Gutknecht (1986).

the second highest. Because of the presence of a hydrophilic and H-bond donor/acceptor group on octanol which is not present on hexadecane, this solvent mimics a chemical environment in between that of the middle of the bilayer and that of the headgroup region.

Even though the chemical selectivity of biomembranes is similar to that of hexadecane and 1-octanol ($s \approx 1$), solute partitioning into lipid bilayers is somewhat lower than in these bulk solvents. The intercepts of the log-log plots for the z-depths reported in Table 1 are all negative. In particular, for hexadecane at $z = 3$ Å the intercept is -0.23 and for 1-octanol at $z = 9.5$ Å the intercept is -1.13 (these z positions are those with s closest to 1). Such findings are also reported in the literature (Marqusee and Dill, 1986).

It is also noted that for log $K(z)$ versus log K(water→hexadecane) the slope is systematically <1, whereas for log $K(z)$ versus log K(water→octanol) the slope is generally >1. A slope <1 indicates that the lipid bilayer is more polar than hexadecane, and a slope >1 indicates that the lipid bilayer is less polar than 1-octanol. Identical findings are reported in experiments (Xiang and Anderson, 1998a), suggesting the simulations are correct. This also explains why the value of s increases for both reference solvents when moving toward the bilayer center. The conclusion is that, on average, the polarity of the lipid bilayer is somewhere in between that of octanol and that of hexadecane.

Barclay-Butler constants

Both experiments (Katz and Diamond, 1974; Simon et al., 1977; Stone, 1975; Jain and Wray, 1977; Simon and Gutknecht, 1980; Smith et al., 1981; De Young and Dill, 1988) and theoretical models (Simon et al., 1979; Katz et al., 1983; Marqusee and Dill, 1986) support the hypothesis that solute partition into bulk organic solvents is not a good model of solute partition into lipid bilayers and biomembranes, primarily from an entropic point of view. The Barclay-Butler constants a and b relate the entropy ΔS and the enthalpy ΔH of solution of different solutes in a given solvent (Katz et al., 1983):

$$\Delta S = a + b\Delta H. \tag{8}$$

A large b constant characterizes a solvent in which entropy changes are relatively more important than enthalpic effects. The fact that in experimental water/membrane partitioning studies the b constant has a larger value than in bulk organic liquids shows that solubilization into membranes is affected to a larger extent by entropic factors. These may arise either from the interfacial constraints of membrane systems, or from the distribution of membrane free volume. Even for noble gases b has a higher value in membranes than in organic solvents. It can therefore be suggested that the similar selectivities of lipid bilayers and some organic solvents only occurs because of a fortunate choice (Katz et al., 1983): the enthalpic effect in a solvent is compensated by the entropic factors in the lipid bilayer.

CORRELATIONS BETWEEN SOLUTE DIFFUSION AND BILAYER PROPERTIES

Unlike experiments, MD simulations allow for the calculation of solute diffusion coefficients in different regions of a lipid bilayer. Possible correlations between its value and bilayer structural and dynamic properties can be investigated.

Correlations between solute diffusion and bilayer free volume

From these simulations there is no strong correlation between solute diffusion coefficients and free volume distribution along the bilayer normal. This is shown at the top of Fig. 1, where the relative diffusion coefficients—i.e., $D(z)/D(30.5)$—are plotted versus free volume percentage along the bilayer normal.

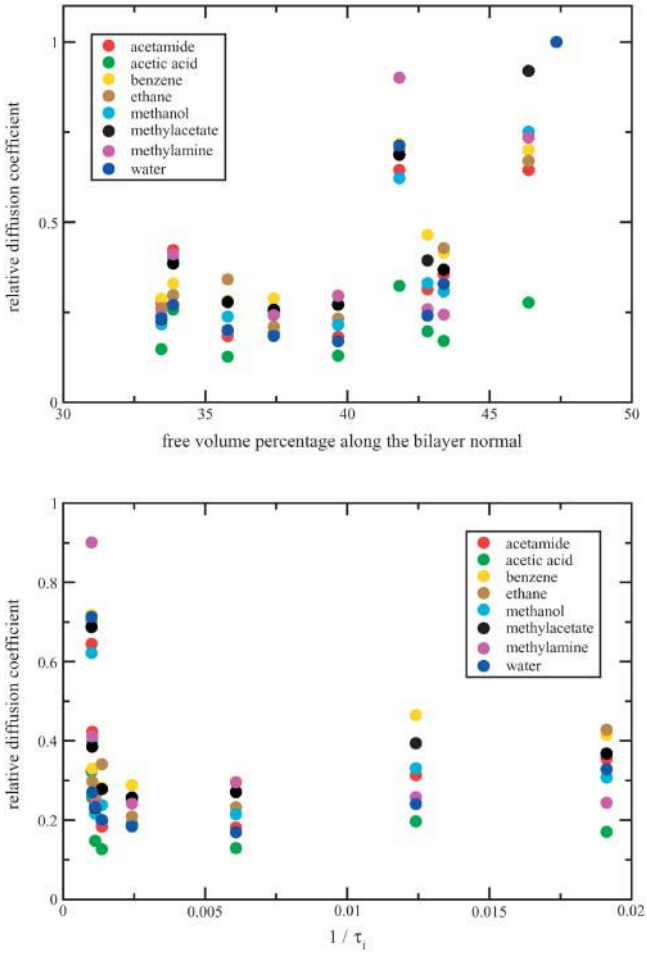

FIGURE 1 (*Top*) Relative diffusion coefficients versus free volume percentage; the former are D-values divided by D at 30.5 Å from the bilayer center (which is in bulk water). (*Bottom*) Relative diffusion coefficients versus the inverse of lipid *trans*/*gauche* interconversion times.

The free volume along the bilayer normal is calculated by searching for vacuum space points in bilayer slabs of 0.5 Å along the bilayer normal, using a grid point spacing of 0.5 Å in the plane of the bilayer. Vacuum points were defined as space points outside the van der Waals radii of the water and lipid molecules. The latter is considered to equal half the parameter σ in the LJ potential for each atom in the system, since σ is the distance at which the LJ energy is zero. The free volume distribution from a 1-ns simulation of a hydrated phospholipid bilayer is presented in Fig. 2.

At a distance further than 27 Å from the bilayer center, which is in the bulk water phase, the free volume percentage for this system is ~47%, in agreement with the percentage that can be calculated analytically from the density of bulk water. Inside the membrane, the lowest free volume is found in region 2 and the highest in region 4, in accordance with the original publication dividing the lipid membrane into the four regions (Marrink and Berendsen, 1994; Marrink et al., 1996). However, those simulations were performed at a higher temperature (350 K) than that used here (323 K) and employed a united-atom model, i.e., with no hydrogens along the lipid tails. Those simulations yielded a higher free volume percentage, above all in the membrane interior: the free volume in region 4 was even higher than in bulk water phase. From this simulation, the lowest free volume percentage is ~32% and the highest is ~43%. Berendsen and co-workers obtained essentially the same value in region 2 (~34%), but a higher percentage in region 4 (~55%). They therefore concluded that the density of region 4 equals that of bulk hexane. This is not true for the membrane model simulated here. Unfortunately, to our knowledge, the free volume distribution along a lipid bilayer normal is not accessible by experiments, and the publications using the CHARMM force field do not report a free volume analysis. The only correlation between diffusion coefficient and free volume is that *D*-values decrease on entering the membrane and are only slightly higher in the bilayer center. The lack of any correlation can be explained on the basis that free volume is rarely sufficient to ensure the presence of holes large enough to accommodate the solutes. Such a lack of correlation was previously reported in the simulation of a drug analog in a lipid bilayer (Alper and Stouch, 1995).

For clarity, it should be noted that the disagreement regarding the lipid bilayer density between this and previous publications is only for the free volume distribution. For the electron density profiles, which are obtained experimentally, both these and previous simulations are in good agreement with the experimental data (Nagle et al., 1996; Nagle and Tristram-Nagle, 2000). Electron densities in simulations are calculated assuming atom-centered electron clouds, whereas the free volume depends on the atomic van der Waals radii defined in the force field. A typical electron density profile obtained from these simulations is reported in Fig. 3. In this case, the lowest density is indeed located in the bilayer core (~0.25 e/Å^3) and the highest density at the lipid/water interface (~0.44 e/Å^3), with the bulk water phase in the middle (~0.33 e/Å^3). Simulations also allow for the unphysical separation of the lipid and water contributions. The two peaks correspond to the electron-rich phosphate fragments and the peak-to-peak distance is well within the experimental range (between 36.4 and 39.6 Å; Nagle et al., 1996; Nagle and Tristram-Nagle, 2000). Thus the differences in the free volume distribution arise either from the force field, or from the method of free volume calculation, relying, as it does, on the atomic van der Waals radii.

Correlations between solute diffusion and lipid internal motions

It is suggested (Xiang, 1998) that diffusion in chain-like solvents such as lipid bilayers can be related to the characteristic times τ_i for solvent internal motions such as

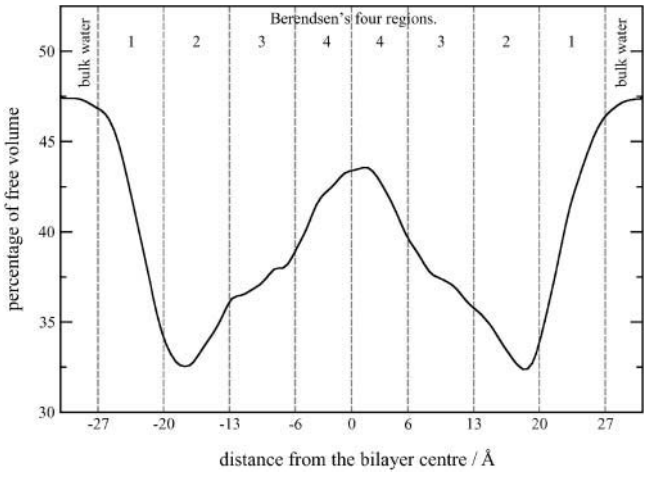

FIGURE 2 Free volume distribution (percentage) along the bilayer normal.

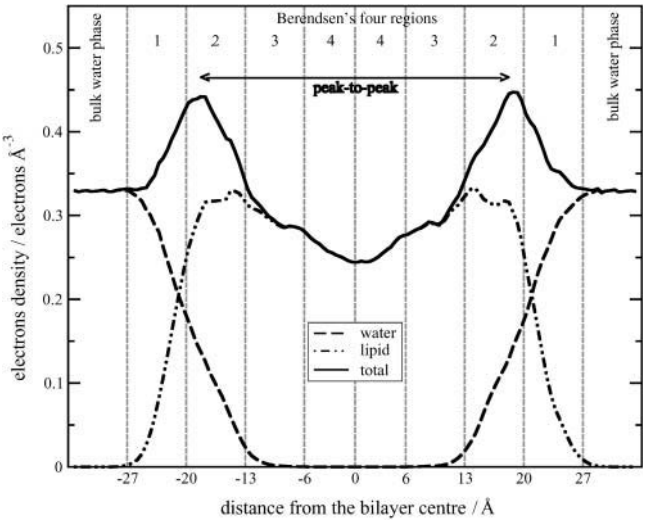

FIGURE 3 Electron density profile.

trans/*gauche* interconversion rates along the lipid hydrocarbon chains. These characteristic times are different at different positions along the lipid chains. A 1-ns simulation of a pure DPPC bilayer performed with the CHARMM force field was analyzed in terms of τ_i, using a convenient time autocorrelation function suggested in the literature (Xiang, 1998):

$$C_\psi(t) = \frac{\langle \cos\psi(t)\cos\psi(0)\rangle - \langle\cos\psi(0)\rangle^2}{\langle\cos^2\psi(0)\rangle - \langle\cos\psi(0)\rangle^2}. \quad (9)$$

Here, ψ is the torsional angle along the lipid tails and the angular brackets denote averages over all the time origins and all the lipids. The results are plotted in Fig. 4.

The curves were fitted with double exponentials

$$C_\psi(t) = C_1\exp(-t/\tau_{short}) + C_2\exp(-t/\tau_{long}). \quad (10)$$

With the exception of the $C(t)$ for the two or three torsions closest to the terminal methyl, the curves do not decay to zero in a time which is short compared with the complete simulation time. Therefore statistics are poor and detailed numerical comparisons of the correlation times are not appropriate. The short decay time τ_{short} can be identified as the motion within the *trans* or *gauche* potential well, and is quite similar for all the torsions, with a value between 20 and 30 ps. The long decay time τ_{long} is associated to the transition between *trans* and *gauche* states and varies along the lipid chain. For the first three torsions, which are those closest to the carbonyl group, its value is longer than 1 ns, which is the total length of the pure DPPC simulation. For torsions 4–8 (assuming torsion 1 is the closest to the carbonyl group and torsion 13 the closest to the terminal methyl group), τ_{long} is between 200 and 300 ps. For torsions 9–11, it is between 60 and 90 ps, and for the last two torsions it is ~20 ps. The characteristic time τ_{long} corresponds to τ_i mentioned above and in what follows.

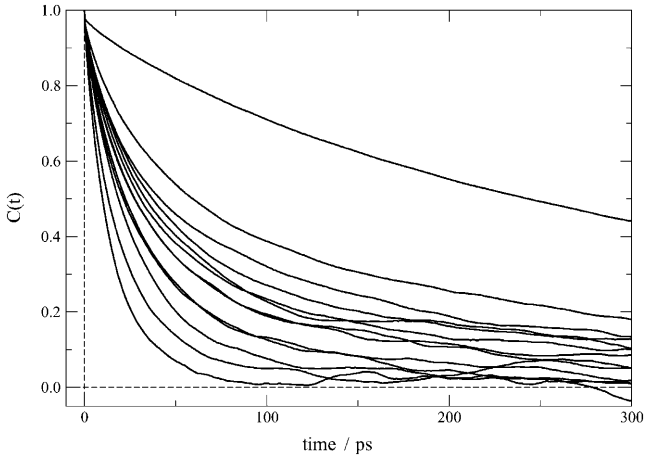

FIGURE 4 Time autocorrelation functions for torsional angles along the lipid tails. The shorter the decay time, the closer to the terminal methyl.

Experimentally, direct measurement of the above correlation times is not possible. Lipid tail motions have been investigated with the measurement of ^2H and ^{13}C spin-lattice relaxation times (Seelig, 1977; Venable et al., 1993; Pastor et al., 1988; Brown et al., 1979). These are thought to be related to lipid motions as a whole, such as the axial rotation and the tilting of the lipid molecule with respect to the bilayer normal, and to lipid internal motions, such as *trans*/*gauche* interconversions. This interpretation leads to the conclusion that, in agreement with simulation results, the mean life of *trans* and *gauche* conformers is of the order of hundreds of picoseconds in the upper part of the lipid chains, and tens of picoseconds in the lower part.

Lipid chain *trans*/*gauche* transitions are thought to be the main mechanism responsible for free volume redistribution inside the membrane, since lipid translation and rotation as a whole require much longer times. This would predict lower solute diffusion in the upper part of the lipid tails, where τ_i is longer, and a higher value at the end of the tails, where τ_i is shorter. Although from these simulations diffusion coefficients in the center of the membrane are slightly higher there is no evident correlation between lipid τ_i and solute D. This is clear from the bottom of Fig. 1, where relative diffusion coefficients are plotted against the inverse of the lipid *trans*/*gauche* interconversion times ($1/\tau_i$). Since there is no correlation between solute D and the free volume distribution, an absence of correlation between solute D and lipid τ_i would also be expected, since τ_i mainly acts to redistribute the free volume. Moreover, the longest decay time of the force autocorrelation function $\langle\Delta\mathbf{F}(z,t)\cdot\Delta\mathbf{F}(z,0)\rangle$ in Eq. 5 (this function was fitted with a double exponential) is ~12 ps, which is shorter than lipid τ_i at all the depths. This suggests that lipid internal flexibility may be only one of several contributions to solute diffusion along the bilayer normal. Although the absence of strong correlation between lipid chain internal dynamics and penetrant diffusion may seem strange, these simulations suggest that for such small solutes these lipid motions are not the only factors affecting their friction.

CORRELATIONS BETWEEN SOLUTE DIFFUSION AND SOLUTE SIZE

Correlations between solute diffusion and solute molecular volume

The solute volume V_d was calculated using the same method applied to calculate the free volume along the bilayer normal. The solute was placed in a reasonably large box, for which points outside the van der Waals radii of the solute atoms were counted. This gave the free volume of the box. The value V_d was then equal to the difference between the total volume of the box and the free volume.

Fig. 5 contains log-log plots of D versus V_d. Investigating the nature of the $D \propto (V_d)^s$ relationship, the slopes of those plots yield the value of the exponent s. In Fig. 5 the distances z from the bilayer center and the slopes s are also reported. The slope at $z = 30.5$ Å, where the solutes are still in bulk water, is in agreement with the experimental observation that $\log(D)$ is approximately $\propto -0.6 \log(V_d)$ (Xiang and Anderson, 1994; Xiang, 1999; Walter and Gutknecht, 1986) for small solutes in sphere-like solvents. With the exception of the D-values 30.5 Å distant from the bilayer center, i.e., in bulk water, for which the correlation coefficient is 0.96, unfortunately the data are quite scattered and correlation coefficients are between 0.59 and 0.86. The interesting feature is that the size dependence of D is only higher than that in water at the interface ($z = 27$ and 23.5 Å), and lower in the membrane interior. It must be said that, although the membrane system is very different, this is in contrast to simulations of a bilayer of fatty acids (Xiang, 1999), where it was found that solute diffusion along the bilayer normal had a greater dependence on solute volume than in bulk water, above all in the upper part of the chains, which are expected to mimic the upper part of the lipid tails in phospholipid bilayers. That result was confirmed by the experimental observation that diffusion in long-chain alkanes and polymers shows a greater dependence on solute size than in simple liquids (Xiang, 1999). However, in those simulations the solutes studied were simple spherical particles representing noble gases, whereas in the simulations reported here much more complex shapes are involved.

Correlations between solute diffusion and solute mass

The dependence of D on solute mass was also studied. Log-log plots are reported in Fig. 6 with the same conventions as in Fig. 5. It is comforting to see that $D(30.5)$, which is the

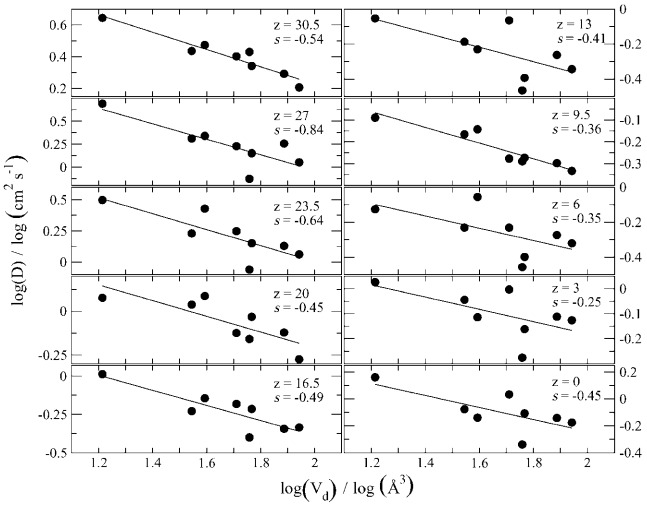

FIGURE 5 Log-log plots of diffusion coefficients as a function of solute volume at different z-depths (in Å) in the membrane. Solid lines are linear regression. The s-slopes are also reported.

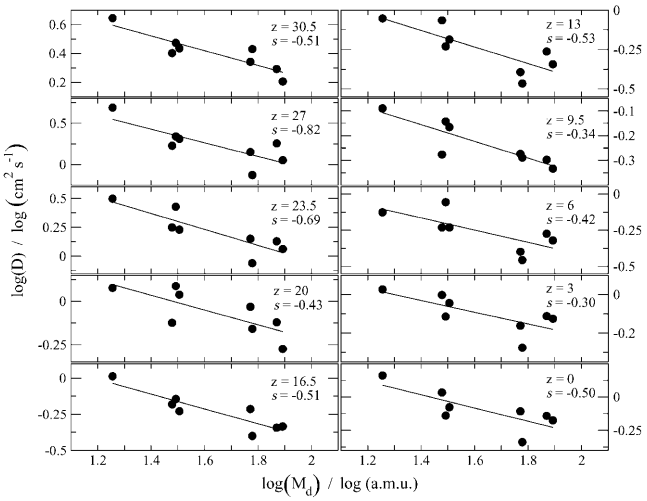

FIGURE 6 Log-log plots of diffusion coefficients as a function of solute mass at different z-depths (in Å) in the membrane. Solid lines are linear regression. The s-slopes are also reported.

diffusion coefficient in bulk water, has $s \approx -1/2$ in excellent agreement with experimental observations for small molecules diffusing in water (Lieb and Stein, 1969, 1971; Xiang and Anderson, 1994; Walter and Gutknecht, 1986). The trend found for the log D-log V_d relationship is also found for the log D-log M relationship: higher s-values at the interface and then lower values inside the membrane, with respect to the water phase. This is in contrast with the experimental observation that diffusion coefficients in polymers and cell membranes have a higher mass-dependence than in simple liquids (Lieb and Stein, 1969, 1971; Wolosin et al., 1978; Stein, 1981; Xiang and Anderson, 1994; Walter and Gutknecht, 1986). These studies led to the conclusion that diffusion in biological membranes resembles that in soft polymers and depends on the formation frequency and the size distribution of pockets of free space among which solutes can jump. The simulations performed here do not support these results derived from polymers and cell membranes. This aspect is pursued in more detail later.

Experiments versus simulations

The assumptions associated with the experiments that determine the solute diffusion dependence on both solute mass M and volume V_d must be assessed. The main limitation of these experiments resides in the fact that diffusion coefficients across the membrane are not accessible directly, but rather they must be extrapolated from the measurement of the permeability coefficients. According to the solubility-diffusion model, assuming the main resistance to permeation comes from a uniform distinct barrier region in the membrane, the solute permeability coefficient can be expressed as a function of the solute partition coefficient and diffusion coefficient inside the barrier region and the

thickness of that region, Eq. 2. To study the dependence of D on solute M or V_d, the logarithm of the ratio between the experimentally measured permeability coefficient P across membranes and the partition coefficient K in organic solvent/water systems, $\log(P/K)$, is plotted versus $\log(M)$ or $\log(V_d)$ (Lieb and Stein, 1969; Walter and Gutknecht, 1986; Xiang and Anderson, 1994). K in organic solvent/water systems is used as an estimation of K in the membrane barrier region. This ascribes the entire molecular size-dependence in P to the diffusion coefficient and neglects the possibility of size-dependent solute partitioning. It was found (Xiang and Anderson, 1994) that changing reference organic solvent or using models that ascribe the size dependence of P to both partitioning and diffusive behaviors decreases the slopes s to values much closer to that in simple liquids (-0.5), although still higher. This suggests that the size dependence of diffusion in lipid bilayers may be less than previously thought, and thus closer to the results of these simulations. Finally, it must not be forgotten that these simulations are limited to solutes with similar size and exclude large molecules like nucleosides or steroids, which are included in the interpretation of the experimental results.

Correlations between solute diffusion and solute cross-sectional area

Finally, it has been suggested (Xiang, 1998) that diffusion in chain-like solvents is related to the solute cross-sectional area, S_d. In contrast to classical free volume diffusion theories, solute displacement can occur not only when a void of volume comparable to that of the diffusant is created, but also when the cross-sectional area of the newly created void is equal to or greater than that of the diffusant. This would predict $D \propto (S_d)^s$ with s negative. Since in this lipid system voids, as calculated using the CHARMM atomic van der Waals radii, large enough to locate these solutes have never been found, the dependence of D on S_d appears particularly interesting. In fact, these simulations do show this relation. Solute S_d was calculated here by taking the solutes in their equilibrium conformation, which is the one corresponding to the bonds and angles set to the values used as equilibrium values in the force-field parameters. The size of each atom was then taken from its van der Waals radius in the force field. The molecular side whose area was considered to be the S_d is shown in Fig. 7 for each solute.

Fig. 8 plots solute $\log(D)$ as a function of solute $\log(S_d)$. The solid lines are linear regressions. With the exception of $z = 30.5$ Å, with a value of 0.93, correlation coefficients for these regressions are not high (between 0.71 and 0.87), but this may depend on the low number of data points (eight solutes) and the uncertainties intrinsic in the MD simulation technique. The main feature is that at all depths solute diffusion does depend on solute cross-sectional area, in agreement with previous theories (Xiang, 1998). The diffusion dependence on S_d also appears to be even larger

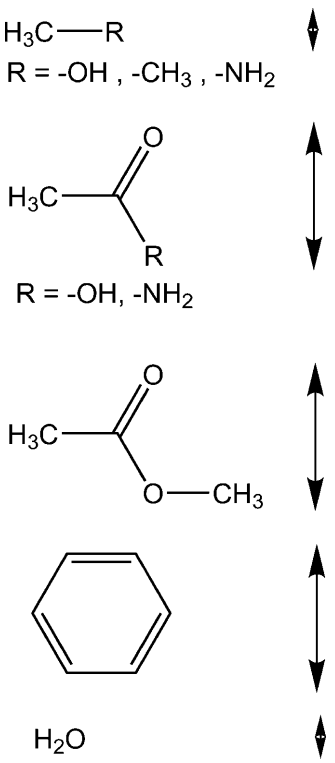

FIGURE 7 Calculation of solute cross-sectional area. The cross-sectional area is calculated as the area observed when looking from the arrows toward the molecules in the plane of the page.

than the dependence on V_d, approximately twice as large. The correlation coefficients are also a little higher. As for the relationship with solute volume and mass, the dependence on S_d inside the membrane is lower than in the water phase, with the exception of the interface.

CORRELATION BETWEEN PERMEABILITY AND PARTITION COEFFICIENT

By analogy with Eq. 7 (which relates the partition coefficient of a solute in two different solvents), and assuming that the main contribution to the permeation resistance comes from a distinct and uniform barrier region inside the lipid bilayer, a linear free energy relationship correlating the permeability coefficient P with the partition coefficient $K_{org/w}$ in a reference organic solvent can be derived (Xiang and Anderson, 1998a, 2000a; Walter and Gutknecht, 1984):

$$\log P = s \log K_{org/w} + i. \quad (11)$$

The slope s measures the relative chemical affinities of the solutes for the barrier domain in the bilayer versus the organic solvent chosen for the correlation. The solvent yielding $s = 1$ in Eq. 11 exactly matches the chemical selectivity of the bilayer barrier domain (Xiang and Anderson, 1998a, 2000a).

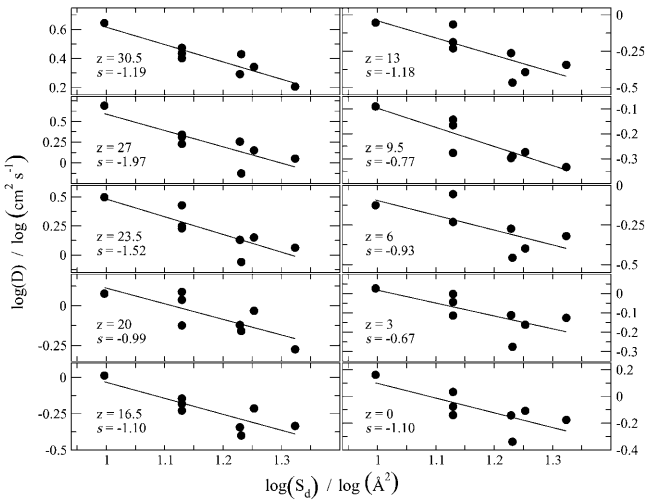

FIGURE 8 Log-log plot of diffusion coefficients as a function of solute cross-sectional areas S_d at different z-depths (in Å) in the membrane. The s-values are slopes of linear regressions.

From experiments, many solvents yield fairly good results. Depending on the set of solutes, the type of membrane, and the method employed to measure P and $K_{org/w}$, some authors have found that the solvents yielding s closest to 1 are saturated long-chain hydrocarbons like hexadecane (Finkelstein, 1976; Orbach and Finkelstein, 1980; Walter and Gutknecht, 1984, 1986), confirming that the main barrier to permeation is the hydrocarbon core of the lipid bilayer, whereas some others have had better results with more polar/polarizable solvents like unsaturated hydrocarbons (Xiang and Anderson, 1994, 1995, 1997, 1998a), suggesting that the barrier domain is probably located closer to the interface. These empirical observations are in accordance with Overton's rule (Overton, 1895), which states that solute permeability is correlated with solute partitioning in oil/water systems.

These simulations allow for the direct calculation of K at every depth of the lipid bilayer, so no reference solvent is needed. The K-values obtained with Eq. 4 from the z-depths that yield the highest $\Delta G(z)$ or R(z) values should be equivalent to the K-values in the solvent that best mimic the barrier region of the lipid bilayer. However, plotting the logarithm of P-values obtained from these simulations versus the logarithm of the above defined K-values yields $s \approx 0.88$, with a correlation coefficient higher than 0.99. If K in hexadecane are employed instead, $s \approx 0.50$, with a correlation coefficient $\approx$0.90.

The failure to reproduce the experimental observation ($s \approx 1$) by these simulations may be explained by the low number of solutes studied here and by the uncertainties intrinsic in the MD simulations. Moreover, in experiments, the resistance profile is approximated to a rectangular shape: the resistance is zero outside the barrier domain and at a constant value >0 inside the barrier. These simulations instead reveal that the shape is far more complicated and smooth, and the width of the barrier region is quite different for different solutes (Bemporad et al., 2004). Therefore, considering the partition at the z-depth with the highest $\Delta G(z)$ or R(z) is an oversimplification which does not hold for the permeability coefficients calculated from these simulations. This result does not imply, however, that in the experiments the choice of a good reference organic solvent yielding $s = 1$ is not a reasonable model for the barrier opposing solute permeation.

PERMEABILITY DEPENDENCE ON MOLECULAR SIZE

As mentioned in the subsection Experiments versus Simulations, direct measurement of diffusion coefficients inside the membrane from experiment is not possible. To study the dependence of D on solute size, the logarithm of the ratio between the experimentally measured permeability coefficient P across membranes and the partition coefficient K in an organic solvent/water systems, log(P/K), is plotted versus log(M) or log(V_d) (Lieb and Stein, 1969; Walter and Gutknecht, 1986; Xiang and Anderson, 1994). The value K in organic solvent/water systems is used as an estimation of K in the membrane barrier region. According to Eq. 1, the ratio between permeability and partition coefficients, the so-called hydrophobicity-corrected permeability, yields the value of the solute diffusion coefficient D in the membrane barrier region, divided by the barrier region thickness d. The same approach to study permeability size-dependence is used here. Fig. 9 contains the log-log plots of the ratios between permeability coefficients as calculated from these simulations and experimental partition coefficients in hexadecane versus solute mass M, volume V_d, and cross-

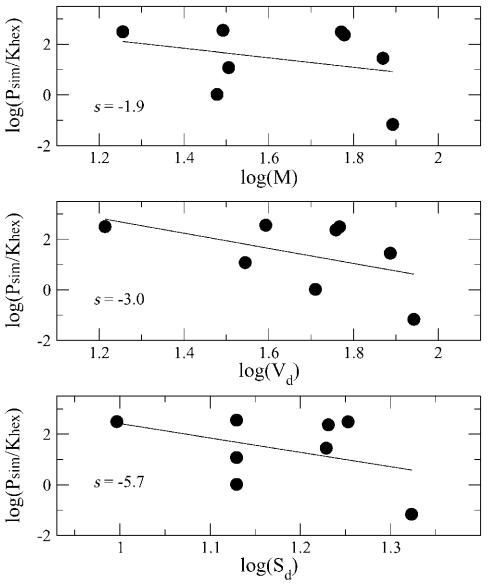

FIGURE 9 Log-log plots of permeability-partition ratio versus solute mass M, volume V_d, and cross-sectional area S_d. The s-values are slopes of linear regressions.

sectional area S_d. The s-values reported in these graphs are the slopes of linear regressions. That is the exponent in the relationship

$$\frac{P}{K} = \frac{D}{d} \propto A^s, \tag{12}$$

where A is a solute property related to the size, i.e., mass M or volume V_d or cross-sectional area S_d.

The correlation coefficients for these plots are low, $\approx$0.4. Correlation coefficients from some experiments are very low too, varying between 0.12 and 0.70 (Walter and Gutknecht, 1986; Xiang and Anderson, 1994) depending on the choice of solutes and reference solvent employed for K. The reason for the poor correlation from the simulations may reside in the low number of data points (eight solutes, whereas in experiments more than 20 solutes are examined—Lieb and Stein, 1969; Walter and Gutknecht, 1986; Xiang and Anderson, 1994), in the narrow range of sizes of the solutes studied (some experiment also includes large molecules such as nucleosides and steroids; Xiang and Anderson, 1994), and in the uncertainties intrinsic to the simulations. However, in Fig. 9 there is the indication of a correlation between solute size and P/K ratios. Thus, although the correlation is too poor here to conclude anything significant, the experimental trend is broadly reproduced. This observation has led experimental scientists to think that the diffusive behavior inside the membrane is strongly dependent on solute size, more than it is in water or simple liquids, and rather similar to that in synthetic polymers.

These simulations allow for the direct calculation of partition coefficients K at every depth of the lipid bilayer. Instead of K in hexadecane, if one uses in the above Eq. 12 the K-values obtained with Eq. 4 from the z-depths that yield the highest $\Delta G(z)$ or R(z), correlation coefficients for the $\log(P/K)$ versus $\log(M)$ or $\log(V_d)$ plots are only slightly better ($\approx$0.5), although slopes are ≈ -0.6.

The following conclusion can be drawn here. Although correlation coefficients are low, the simulations reproduce the experimental findings that $\log(P/K)$ versus $\log(M)$ or $\log(V_d)$ yields negative slopes with magnitude $>$0.6. However, when using ''real'' K-values between the water and the lipid bilayer, instead of the K-values in a bulk organic solvent like hexadecane, a much smaller size dependency is obtained. This agrees with the $D(z)$ versus $\log(M)$ or $\log(V_d)$ plots (see the subsections Correlations Between Solute Diffusion and Solute Size and Correlations Between Solute Diffusion and Solute Mass), which yield low slopes. Therefore, the experimental approach using K in bulk solvents overestimates the size dependence of diffusion coefficients inside the membrane.

IMPLICATIONS FOR DRUG DESIGN

As mentioned in the Introduction, the study of membrane permeation is relevant for drug design. The simulations described here can help in at least two aspects. First, they model with atomic detail the permeation process and can help in the interpretation of experiments. Second, they suggest an alternative for the observed size dependence of that process. Drug design makes routine use of partition coefficient measurements in water/organic solvent systems to estimate the ability of a drug to cross biological membrane and finally to be absorbed after administration. Based on the results of these simulations, a correction factor could be added to those partition coefficients when correlated to absorption data, to take into account the different behavior of biomembranes and bulk solvents. This could include the higher size dependence and the presence of entropic factors in lipid bilayer systems, as noted in the previous sections. The simulations of small organic solutes like those reported here cannot help drug design directly, because drugs are much bigger and more flexible molecules, but they can reveal general properties of the permeation mechanism. Moreover, the methodology described in this article can now be considered successfully tested, and can be further employed in the simulation of real drug molecules. Such work has been carried out and will be the subject of a separate article.

CONCLUSIONS

In this article, all-atom MD simulations have been used to investigate the local partitioning and diffusion of small organic compounds in a lipid bilayer membrane. Results suggest that calculated diffusion coefficients inside the bilayer are dependent on solute size to a lesser extent than in water or simple liquids. This is not in contrast with the experimental observation that the ratio of permeability coefficients across biological membranes and partition coefficients in reference organic solvents has a strong dependence on solute size, because this trend is reproduced by the simulations. However, it is in contrast with the interpretation of that experimental observation, which ascribes the size dependence to the solute diffusion only. From these simulations, the size dependence shown by permeability is instead to be ascribed to the partitioning behavior of the solutes into the lipid bilayer. This is confirmed by the fact that the size dependence of the permeability/partition ratio significantly decreases when using partition coefficients inside the bilayer instead of those in bulk solvent. Moreover, the fact that $\log K$(membr)–$\log K$(water/hexadecane,water/octanol) plots have negative intercepts show that solute partitioning into lipid bilayers is lower than in bulk solvents. These simulations clearly show with an atomic detail that the membrane core does not behave like a simple slab of bulk solvent.

The authors thank I. C. Walton, I. D. Hardy, and O. G. Parchment for their help in running the simulations on the Southampton University PC cluster called IRIDIS (http://www.sucs.soton.ac.uk/research/iridis/).

We thank the Engineering and Physical Sciences Research Council for supporting this work, and D.B. thanks Aventis for its generous support.

REFERENCES

Alper, H. E., and T. R. Stouch. 1995. Orientation and diffusion of a drug analog in biomembranes—molecular dynamics simulations. *J. Phys. Chem.* 99:5724–5731.

Balaz, S. 2000. Lipophilicity in trans-bilayer transport and subcellular pharmacokinetics. *Perspect. Drug Discov. Des.* 19:157–177.

Bar-On, Z., and H. Degani. 1985. Permeability of alkylamines across phosphatidylcholine vesicles as studied by H-NMR. *Biochim. Biophys. Acta.* 813:207–217.

Bassolino-Klimas, D., H. E. Alper, and T. R. Stouch. 1993. Solute diffusion in lipid bilayer-membranes—an atomic-level study by molecular dynamics simulation. *Biochemistry.* 32:12624–12637.

Bassolino-Klimas, D., H. E. Alper, and T. R. Stouch. 1995. Mechanism of solute diffusion through lipid bilayer-membranes by molecular dynamics simulation. *J. Am. Chem. Soc.* 117:4118–4129.

Bean, R. C., W. C. Shepherd, and H. Chan. 1968. Permeability of lipid bilayer membranes to organic solutes. *J. Gen. Physiol.* 52:495–508.

Bemporad, D., J. W. Essex, and C. Luttmann. 2004. Permeation of small molecules through a lipid bilayer: a computer simulation study. *J. Phys. Chem. B.* 108:4875–4884.

Berendsen, H. J. C., and S. J. Marrink. 1993. Molecular dynamics of water transport through membranes: water from solvent to solute. *Pure Appl. Chem.* 65:2513–2520.

Bochain, A., L. Estey, G. Haronian, M. Reale, C. Rojas, and J. Cramer. 1981. Determination of catecholamine permeability coefficients for passive diffusion across phospholipid vesicle membranes. *J. Membr. Biol.* 60:73–76.

Bresseleers, G. J. M., H. L. Goderis, and P. P. Tobback. 1984. Measurement of the glucose permeation rate across phospholipid bilayers using small unilamellar vesicles. *Biochim. Biophys. Acta.* 772:374–382.

Brooks, B. R., R. E. Bruccoleri, B. D. Olafson, D. J. States, S. Swaminathan, and M. Karplus. 1983. CHARMM—a program for macromolecular energy, minimization, and dynamics calculations. *J. Comp. Chem.* 4:187–217.

Brown, M., J. Seelig, and U. Haberlein. 1979. Structural dynamics in phospholipid bilayers from deuterium spin-lattice relaxation time measurements. *J. Chem. Phys.* 70:5045–5053.

Brunner, J., D. E. Graham, H. Hauser, and G. Semenza. 1980. Ion and sugar permeabilities of lecithin bilayers: comparison of curved and planar bilayers. *J. Membr. Biol.* 57:133–141.

Cascales, J. J. L., J. G. H. Cifre, and J. G. de la Torre. 1998. Anaesthetic mechanism on a model biological membrane: a molecular dynamics simulation study. *J. Phys. Chem. B.* 102:625–631.

Cohen, B. E. 1975a. The permeability of liposomes to nonelectrolytes. I. Activation energies for permeation. *J. Membr. Biol.* 20:205–234.

Cohen, B. E. 1975b. The permeability of liposomes to nonelectrolytes. II. The effect of nystatin and gramicidin A. *J. Membr. Biol.* 20:235–268.

De Young, L. R., and K. A. Dill. 1988. Solute partitioning into lipid bilayer membranes. *Biochemistry.* 27:5281–5289.

Diamond, J. M., and Y. Katz. 1974. Interpretation of nonelectrolyte partition coefficients between dimyristoyl lecithin and water. *J. Membr. Biol.* 17:121–154.

Dix, J. A., D. Kivelson, and J. M. Diamond. 1978. Molecular motion of small nonelectrolyte molecules in lecithin bilayers. *J. Membr. Biol.* 40:315–342.

Feller, S. E., and R. W. Pastor. 1996. On simulating lipid bilayers with an applied surface tension: periodic boundary conditions and undulations. *Biophys. J.* 71:1350–1355.

Feller, S. E., and R. W. Pastor. 1999. Constant surface tension simulations of lipid bilayers: the sensitivity of surface areas and compressibilities. *J. Chem. Phys.* 111:1281–1287.

Feller, S. E., R. M. Venable, and R. W. Pastor. 1997. Computer simulation of a DPPC phospholipid bilayer: structural changes as a function of molecular surface area. *Langmuir.* 13:6555–6561.

Feller, S. E., Y. Zhang, R. W. Pastor, and B. R. Brooks. 1995. Constant pressure molecular dynamics simulation: the Langevin piston. *J. Chem. Phys.* 103:4613–4621.

Finkelstein, A. 1976. Water and nonelectrolyte permeability of lipid bilayer membranes. *J. Gen. Physiol.* 68:127–135.

Gutknecht, J., and A. Walter. 1981. Histamine, theophylline and tryptamine transport through lipid bilayer membranes. *Biochim. Biophys. Acta.* 649:149–154.

Hill, W. G., R. L. Rivers, and M. L. Zeidel. 1999. Role of leaflet asymmetry in the permeability of model biological membranes to protons, solutes, and gases. *J. Gen. Physiol.* 114:405–414.

Hockney, R. W. 1970. The potential calculation and some applications. *Meth. Comp. Phys.* 9:136–211.

Hoover, W. G. 1985. Canonical dynamics: equilibrium phase-space distributions. *Phys. Rev. A.* 31:1695–1697.

Jain, M. K., and L. V. Wray, Jr. 1977. Partition coefficients of alkanols in lipid bilayer/water. *Biochem. Pharma.* 27:1294–1296.

Katz, Y., and J. M. Diamond. 1974. Thermodynamic constants for non-electrolyte partition between dimyristoyl lecithin and water. *J. Membr. Biol.* 17:101–120.

Katz, Y., M. E. Hoffman, and R. Blumenthal. 1983. Parametric analysis of membrane characteristics and membrane structure. *J. Theor. Biol.* 105:493–510.

Koubi, L., M. Tarek, M. L. Klein, and D. Scharf. 2000. Distribution of halothane in a dipalmitoylphosphatidylcholine bilayer from molecular dynamics calculations. *Biophys. J.* 78:800–811.

Lande, M. B., J. M. Donovan, and M. L. Zeidel. 1995. The relationship between membrane fluidity and permeabilities to water, solutes, ammonia and protons. *J. Gen. Physiol.* 106:67–84.

Lieb, W. R., and W. D. Stein. 1969. Biological membranes behave as non-porous polymeric sheets with respect to the diffusion of non-electrolytes. *Nature.* 224:240–243.

Lieb, W. R., and W. D. Stein. 1971. The molecular basis of simple diffusion within biological membranes. *Curr. Top. Membr. Transp.* 2:1–39.

MacKerell, A. D., and S. E. Feller. 2000. An improved empirical potential energy function for molecular simulations of phospholipids. *J. Phys. Chem. B.* 104:7510–7515.

Marqusee, J. A., and K. A. Dill. 1986. Solute partitioning into chain molecule interphases: monolayers, bilayers membranes and micelles. *J. Chem. Phys.* 85:434–444.

Marrink, S. J., and H. J. C. Berendsen. 1994. Simulation of water transport through a lipid-membrane. *J. Phys. Chem.* 98:4155–4168.

Marrink, S. J., and H. J. C. Berendsen. 1996. Permeation process of small molecules across lipid membranes studied by molecular dynamics simulations. *J. Phys. Chem.* 100:16729–16738.

Marrink, S. J., R. M. Sok, and H. J. C. Berendsen. 1996. Free volume properties of a simulated lipid membrane. *J. Chem. Phys.* 104:9090–9099.

Nagle, J. F., and S. Tristram-Nagle. 2000. Structure of lipid bilayers. *Biochim. Biophys. Acta. Rev. Biomembr.* 1469:159–195.

Nagle, J. R., R. Zhang, S. Tristram-Nagle, W. Sun, H. Petrache, and R. M. Suter. 1996. X-ray structure determination of fully hydrated L_α-phase dipalmitoylphosphatidylcholine bilayers. *Biophys. J.* 70:1419–1431.

Orbach, E., and A. Finkelstein. 1980. The nonelectrolyte permeability of planar lipid bilayer membranes. *J. Gen. Physiol.* 75:427–436.

Overton, E. 1895. Uber die osmotischen eigenshaften der lebenden pflanzen und tierzellen. *Vierteljahrschr. Naturforsch. Ges. Zurich.* 40:159–201.

Pastor, R. W., R. M. Venable, M. Karplus, and A. Szabo. 1988. A simulation based model of NMR t_1 relaxation in lipid bilayer vesicles. *J. Chem. Phys.* 89:1128–1140.

Paula, S., A. G. Volkov, A. N. Van Hoek, T. H. Haines, and D. W. Deamer. 1996. Permeation of protons, potassium ions, and small polar molecules through phospholipid bilayers as a function of membrane thickness. *Biophys. J.* 70:339–348.

Pohorille, A., M. H. New, K. Schweighofer, and M. A. Wilson. 1999. Insights from computer simulations into the interaction of small molecules with lipid bilayers. *Curr. Top. Membr.* 48:49–76.

Pohorille, A., and M. A. Wilson. 1996. Excess chemical potential of small solutes across water-membrane and water-hexane interfaces. *J. Chem. Phys.* 104:3760–3773.

Pratt, L. R., and A. Pohorille. 2002. Hydrophobic effects and modeling of biophysical aqueous solution interfaces. *Chem. Rev.* 102:2671–2692.

Ryckaert, J. P., G. Ciccotti, and H. J. C. Berendsen. 1977. Numerical integration of the Cartesian equations of motion of a system with constraints: molecular dynamics of *n*-alkanes. *J. Comp. Phys.* 23:327–341.

Seelig, J. 1977. Deuterium magnetic resonance: theory and application to lipid membranes. *Q. Rev. Biophys.* 10:353–418.

Simon, S. A., and J. Gutknecht. 1980. Solubility of carbon dioxide in lipid bilayer membranes and organic solvents. *Biochim. Biophys. Acta.* 596:352–358.

Simon, S. A., W. L. Stone, and P. B. Bennet. 1979. Can regular solution theory be applied to lipid bilayer membranes? *Biochim. Biophys. Acta.* 550:38–47.

Simon, S. A., W. L. Stone, and P. Busto-Latorre. 1977. A thermodynamic study of the partition of *n*-hexane into phosphatidylcholine and phosphatidylcholine-cholesterol bilayers. *Biochim. Biophys. Acta.* 468:378–388.

Singer, S., and G. L. Nicolson. 1972. The fluid mosaic model of cell membranes. *Science.* 172:720–730.

Smith, R. A., E. G. Porter, and K. W. Miller. 1981. The solubility of anesthetic gases in lipid bilayers. *Biochim. Biophys. Acta.* 645:327–338.

Stein, W. D. 1981. Permeability for lipophilic molecules. *In* Membrane Transport. S. L. Bonting and J. H. M. de Pont, editors. Elsevier/North-Holland Biomedical, New York.

Stone, W. L. 1975. Hydrophobic interaction of alkanes with liposomes and lipoproteins. *J. Biol. Chem.* 250:4368–4370.

Stouch, T. R., H. E. Alper, and D. Bassolino. 1995. Simulations of drug diffusion in biomembranes. *Comp. Aided Mol. Des.* 589:127–138.

Todd, A. P., R. J. Mehlhorn, and R. I. Macey. 1989. Amine and carboxylate spin probe permeability in red cells. *J. Membr. Biol.* 109:41–52.

Tu, K., M. Tarek, M. L. Klein, and D. Scharf. 1998. Effects of anesthetics on the structure of a phospholipid bilayer: molecular dynamics investigation of halothane in the hydrated liquid crystal phase of dipalmitoylphosphatidylcholine. *Biophys. J.* 75:2123–2134.

Venable, R. M., Y. Zhang, B. J. Hardy, and R. W. Pastor. 1993. Molecular dynamics simulations of a lipid bilayer and of hexadecane: an investigation of membrane fluidity. *Science.* 262:223–226.

Walter, A., and J. Gutknecht. 1984. Monocarboxylic acid permeation through lipid bilayer membranes. *J. Membr. Biol.* 77:255–264.

Walter, A., and J. Gutknecht. 1986. Permeability of small nonelectrolytes through lipid bilayer membranes. *J. Membr. Biol.* 90:207–217.

Wolosin, J. M., and H. Ginsburg. 1975. The permeation of organic acids through lecithin bilayers resemblance to diffusion in polymers. *Biochim. Biophys. Acta.* 389:20–33.

Wolosin, J. M., H. Ginsburg, W. R. Lieb, and W. D. Stein. 1978. Diffusion within egg-lecithin bilayers resembles that within soft polymers. *J. Gen. Physiol.* 71:93–100.

Xiang, T. X. 1998. A novel dynamic free-volume theory for molecular diffusion in fluids and interphases. *J. Chem. Phys.* 109:7876–7884.

Xiang, T. X. 1999. Translational diffusion in lipid bilayers: dynamic free-volume theory and molecular dynamics simulation. *J. Phys. Chem. B.* 103:385–394.

Xiang, T. X., and B. D. Anderson. 1994. The relationship between permeant size and permeability in lipid bilayer membranes. *J. Membr. Biol.* 140:111–122.

Xiang, T. X., and B. D. Anderson. 1995. Phospholipid surface density determines the partitioning and permeability of acetic acid in DMPC:Cholesterol bilayers. *J. Membr. Biol.* 148:157–167.

Xiang, T. X., and B. D. Anderson. 1997. Permeability of acetic acid across gel and liquid-crystalline lipid bilayers conforms to free-surface-area theory. *Biophys. J.* 72:223–237.

Xiang, T. X., and B. D. Anderson. 1998a. The barrier domain for solute permeation varies with lipid bilayer phase structure. *J. Membr. Biol.* 165:77–90.

Xiang, T. X., and B. D. Anderson. 1998b. Influence of chain ordering on the selectivity of dipalmitoylphosphatidylcholine bilayer membranes for permeant size and shape. *Biophys. J.* 75:2658–2671.

Xiang, T. X., and B. D. Anderson. 1998c. Phase structure of binary lipid bilayers as revealed by permeability of small molecules. *Biochim. Biophys. Acta.* 1370:64–76.

Xiang, T. X., and B. D. Anderson. 2000a. Influence of a transmembrane protein on the permeability of small molecules across lipid membranes. *J. Membr. Biol.* 173:187–201.

Xiang, T. X., and B. D. Anderson. 2000b. A quantitative model for the dependence of solute permeability on peptide and cholesterol content in biomembranes. *J. Membr. Biol.* 177:137–148.

Xiang, T. X., X. Chen, and B. D. Anderson. 1992. Transport methods for probing the barrier domain of lipid bilayer membranes. *Biophys. J.* 63: 78–88.

Zhu, T., J. Li, G. D. Hawkins, C. J. Cramer, and D. G. Truhlar. 1998. Density functional solvation model based on CM^2 atomic charges. *J. Chem. Phys.* 109:9117–9133.